

Site-Directed Sulfhydryl Labeling of the Lactose Permease of *Escherichia coli*: N-Ethylmaleimide-Sensitive Face of Helix II[†]

Pushpa Venkatesan,[‡] Zhilin Liu, Yonglin Hu, and H. Ronald Kaback*

Howard Hughes Medical Institute, Departments of Physiology and Microbiology & Molecular Genetics,
Molecular Biology Institute, University of California—Los Angeles, Los Angeles, California 90095-1662

Received February 25, 2000; Revised Manuscript Received June 2, 2000

ABSTRACT: Cys-scanning mutagenesis of helix II in the lactose permease of *Escherichia coli* [Frillingos, S., Sun, J. et al. (1997) *Biochemistry* 36, 269–273] indicates that one face contains positions where Cys replacement or Cys replacement followed by treatment with *N*-ethylmaleimide (NEM) significantly inactivates the protein. In this study, site-directed sulfhydryl modification is utilized in situ to study this face of helix II. [¹⁴C]NEM labeling of 13 single-Cys mutants, including the nine NEM-sensitive Cys replacements, in right-side-out membrane vesicles is examined. Permease mutants with a single-Cys residue in place of Gly46, Phe49, Gln60, Ser67, or Leu70 are alkylated by NEM at 25 °C in 10 min, and mutants with Cys in place of Thr45 and Ser53 are labeled only in the presence of ligand, while mutants with Cys in place of Ile52, Ser56, Leu57, Leu62, Phe63, or Leu65 do not react. Binding of substrate leads to a marked increase in labeling of Cys residues at positions 45, 49, or 53 in the periplasmic half of helix II and a slight decrease in labeling of Cys residues at positions 60 or 67 in the cytoplasmic half. Labeling studies with methanethiosulfonate ethylsulfonate (MTSES) show that positions 45 and 53 are accessible to solvent in the presence of ligand only, while positions 46, 49, 67, and 70 are accessible to solvent in the absence or presence of ligand. Position 60 is also exposed to solvent, and substrate binding causes a decrease in solvent accessibility. The findings demonstrate that the NEM-sensitive face of helix II participates in ligand-induced conformational changes. Remarkably, this membrane-spanning face is accessible to the aqueous phase from the periplasmic side of the membrane. In the following paper in this issue [Venkatesan, P., Hu, Y., and Kaback, H. R. (2000) *Biochemistry* 39, 10656–10661], the approach is applied to helix X.

As demonstrated in the preceding paper in this issue (Venkatesan, P., Kwaw, I., Hu, Y., and Kaback, H. R.), site-directed sulfhydryl labeling in situ is a useful means to study ligand-induced conformational changes in the lactose permease (lac permease)¹ of *Escherichia coli*, as well as the accessibility of specific positions to water. In this paper, the approach is applied to transmembrane helix II (Figure 1).

Although no irreplaceable residues are found in helix II, several findings indicate that one face of this transmembrane domain is important for activity: (i) Cys-scanning mutagenesis of helix II and the flanking loops shows that positions where Cys replacement or Cys replacement followed by treatment with *N*-ethylmaleimide (NEM) significantly inac-

tivates the protein are situated on one face of helix II (1). More specifically, nine single-Cys mutants (T45C, G46C, F49C, S53C, S56C, Q60C, L65C, S67C, and L70C)² are significantly inactivated by the thiol reagent. With the exception of position 65, all the NEM-sensitive positions occupy the same face of helix II, indicating that this face is important for activity. (ii) A number of observations indicate that helix II interacts with the C-terminal half of the permease where four of the six irreplaceable residues are located. Mutation of Asp68 at the cytoplasmic end of helix II abolishes transport activity (2), and many second-site revertants display high activity (3). In 7 of the 18 revertants, the inactive phenotype is suppressed by a mutation in the middle of helix VII; 6 of the 18 revertants are located at the periplasmic end of helix XI. Thiol cross-linking experiments demonstrate that helix II is close to helix VII at the periplasmic face of the membrane and to helix XI at the cytoplasmic face (4–6). Furthermore, ligand binding causes an increase in distance between the periplasmic ends of helices II and VII and a decrease in the distance between the two helices near the middle of the membrane (6), and importantly, iodine-catalyzed cross-linking at the periplasmic

[†] This work was supported in part by NIH Grant DK51131 to H.R.K.

* To whom correspondence should be addressed. HHMI/UCLA, 5-748 MacDonald Research Laboratories, Box 951662, Los Angeles, CA 90095-1662. Telephone: (310) 206–5053. Telefax: (310) 206–8623. E-mail: RonaldK@HHMI.UCLA.edu

[‡] P.V. is the recipient of NIH NRSA Postdoctoral Fellowship 5 F32 DK09287.

¹ Abbreviations: lac permease, lactose permease; Cys-less permease, functional lac permease devoid of Cys residues; TDG, β ,D-galactopyranosyl 1-thio- β ,D-galactopyranoside; NEM, *N*-ethylmaleimide; MTSES, methanethiosulfonate ethylsulfonate; $\Delta\mu_{\text{H}^+}$, the H⁺ electrochemical gradient across the membrane; IPTG, isopropyl 1-thio- β ,D-galactopyranoside; RSO, right-side-out; ISO, inside-out; DTT, dithiothreitol; KP_i, potassium phosphate; DDM, *n*-dodecyl β ,D-maltopyranoside; NaDodSO₄, sodium dodecyl sulfate.

² Site-directed mutants are designated by the single-letter amino acid abbreviation for the targeted residue, followed by the sequence position of the residue in the wild-type lac permease, and followed by a second letter indicating the amino acid replacement.

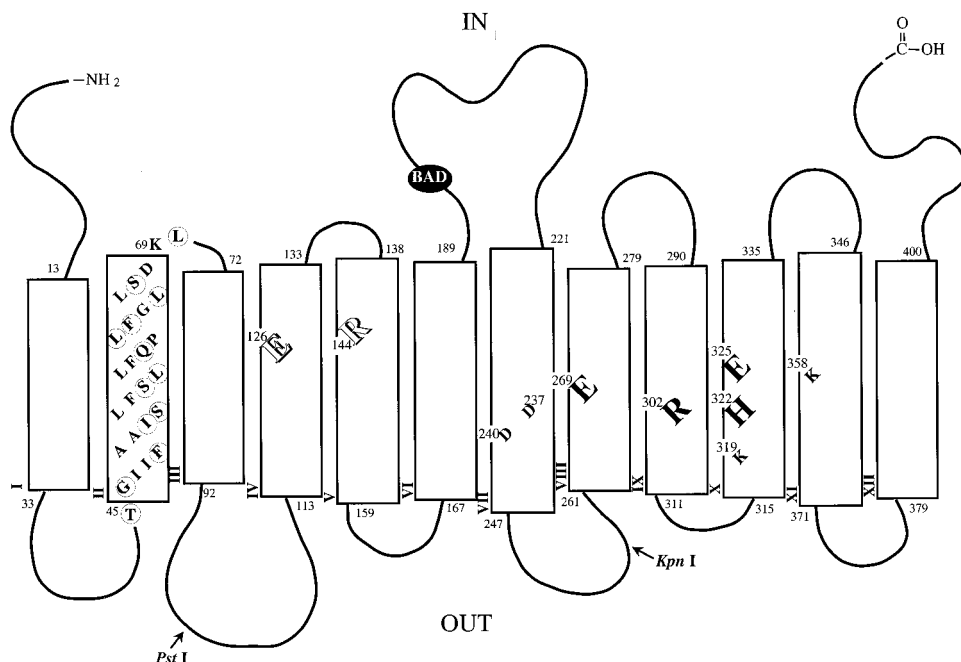


FIGURE 1: Secondary structure model of lac permease. The single-letter amino acid code is used, and putative transmembrane helices are shown in boxes. The six irreplaceable residues Glu126 (helix IV), Arg144 (helix V), Glu269 (helix VIII), Arg302 (helix IX), His322 (helix X), and Glu325 (helix X) are shown as enlarged Roman letters. In addition, the charge pairs Asp237 (helix VII)/Lys358 (helix XI) and Asp240 (helix VII)/Lys319 (helix X) are shown. The residues in helix II studied by site-directed NEM labeling are shown in shaded circles, and the site of the biotin acceptor domain (BAD) is indicated.

ends inactivates transport (5). In addition, periplasmic loop I/II (loop I/II) is proximal to loops VII/VIII and XI/XII (7–9). (iii) The cytoplasmic end of helix II and loop II/III contains the conserved sequence motif $^{64}\text{G-X-X-X-D-(R/K)-X-G-X-(R/K)-(R/K)}$ (10), and insertional mutagenesis of loop II/III (11) or site-specific mutagenesis of Gly64 (12) or Asp68 (2) inactivates the permease.

In this paper, the structural and dynamic role of the NEM-sensitive face of helix II is investigated by site-directed NEM labeling of single-Cys replacement mutants in right-side-out (RSO) membrane vesicles (13–15). The results demonstrate that this face of helix II participates in conformational changes induced by substrate binding, and remarkably, that this membrane-spanning face is accessible to solvent from the periplasmic side of the membrane.

EXPERIMENTAL PROCEDURES

Materials. Materials were obtained from sources described previously (Venkatesan, P., Kwaw, I., Hu, Y., and Kaback, H. R., preceding paper in this issue).

Methods. Plasmid Construction. Construction of permease mutants containing single-Cys replacements at positions 45, 46, 49, 52, 53, 56, 57, 60, 62, 63, 65, 67, and 70 in a Cys-less background has been described (1). To facilitate avidin affinity purification, a biotin acceptor domain was inserted into the middle cytoplasmic loop of each single-Cys mutant by restriction fragment replacement of the DNA fragment from plasmid pKR35/Cys-less *lacY*-L6XB [encoding Cys-less permease with a biotin acceptor domain in cytoplasmic loop VI/VII (7, 16)] into plasmid pT7-5/C-less *lacY* encoding a given single-Cys mutant using the *Pst*I and *Kpn*I restriction sites. Mutations and insertions were verified by sequencing double-stranded plasmid DNA using the dideoxynucleotide termination method (17).

Growth of Bacteria. *E. coli* T184 (*lacY*[−]*Z*[−]) transformed with a plasmid encoding a given mutant was grown as described (Venkatesan, P., Kwaw, I., Hu, Y., and Kaback, H. R., preceding paper in this issue).

Membrane Preparation. RSO membrane vesicles were prepared as described (Venkatesan, P., Kwaw, I., Hu, Y., and Kaback, H. R., preceding paper in this issue).

NEM Labeling. Alkylation with [¹⁴C]NEM and quantification were performed as described (Venkatesan, P., Kwaw, I., Hu, Y., and Kaback, H. R., preceding paper in this issue).

NEM Labeling in the Presence of $\Delta\mu_{\text{H}^+}$. RSO membrane vesicles [0.4 mg of protein in 50 μL of 100 mM KPi (pH 7.5)/10 mM MgSO_4] with a given single-Cys permease mutant were incubated with [¹⁴C]NEM (40 mCi/mmol; 0.4 mM final concentration) in the absence or presence of 20 mM potassium ascorbate and 0.2 mM phenazine methosulfate under oxygen (18) to generate $\Delta\mu_{\text{H}^+}$. Labeling was terminated after 10 min by the addition of 15 mM DTT, and the permease was solubilized, purified, electrophoresed, and analyzed by autoradiography as described (Venkatesan, P., Kwaw, I., Hu, Y., and Kaback, H. R., preceding paper in this issue).

MTSES Labeling. The reactivity of given single-Cys mutants in RSO membrane vesicles toward MTSES was determined as described (Venkatesan, P., Kwaw, I., Hu, Y., and Kaback, H. R., preceding paper in this issue).

Western Blot Analysis. Fractions containing affinity-purified biotinylated permease were analyzed electrophoretically on sodium dodecyl sulfate (NaDodSO₄)/12% polyacrylamide gels, and proteins were electroblotted and quantified as described (Venkatesan, P., Kwaw, I., Hu, Y., and Kaback, H. R., preceding paper in this issue).

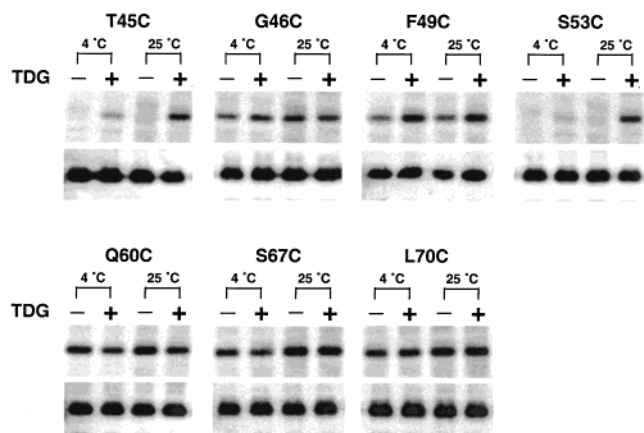


FIGURE 2: Effect of TDG and temperature on NEM labeling of given single-Cys mutants in RSO membrane vesicles. RSO membrane vesicles [0.4 mg of protein in 50 μ L of 100 mM KP_i (pH 7.5)/10 mM MgSO₄] prepared from *E. coli* T184 transformed with a plasmid encoding an indicated single-Cys mutant were incubated with [¹⁴C]NEM (40 mCi/mmol; 0.4 mM final concentration) for 10 min in the absence or presence of 10 mM TDG at 4 or 25 °C as shown. Reactions were terminated with DTT (15 mM final concentration), and biotinylated permease was solubilized and purified by avidin-affinity chromatography as described in Experimental Procedures. Aliquots containing approximately 5 μ g of protein were separated by NaDodSO₄/12% PAGE, and the labeled protein was visualized by autoradiography (upper panels). A fraction of the protein (0.5 μ g) eluted from the avidin-Sepharose beads was analyzed by Western blotting with anti-C-terminal antibody to quantify the amount of permease in each sample (lower panels).

Protein Determinations. Protein was assayed using a Micro BCA protein determination kit (Pierce Inc., Rockford, IL).

RESULTS

NEM Labeling at 25 °C. Mutant G46C, F49C, Q60C, S67C, or L70C reacts with [¹⁴C]NEM in 10 min at 25 °C (Figure 2, lane 3 in the appropriate panel). In contrast, T45C or S53C permease reacts with NEM only in the presence of the high affinity substrate analogue, TDG, (Figure 2, compare lanes 3 and 4 in the appropriate panels), suggesting that binding of substrate elicits a conformational change that causes these Cys side chains to become reactive/accessible to the reagent. A ligand-induced conformational alteration is also reflected at position 49 or 60. Labeling of F49C permease is slightly enhanced, and labeling of Q60C permease is attenuated in the presence of TDG (Figure 2, compare lanes 3 and 4 in the appropriate panels). Labeling of mutants G46C, S67C, or L70C is unchanged in the presence of TDG (Figure 2, compare lanes 3 and 4 in the appropriate panel), implying that conformational changes induced by ligand are either not reflected at these positions or not apparent at 25 °C. No labeling of permease I52C, S56C, L57C, L62C, F63C, or L65C is observed even when incubation with NEM is carried out for 30 min, and with the exception of mutant I52C, which is very weakly labeled in the presence of TDG, ligand has no effect on alkylation of these mutants (data not shown).

NEM Labeling at 4 °C. Labeling with [¹⁴C]NEM was also carried out at 4 °C to minimize thermal motion of the protein and thereby facilitate detection of possible ligand-induced conformational changes (5, 19). Alkylation of G46C permease at 4 °C is comparable to that observed at 25 °C after

normalization for protein (Figure 2, G46C, compare lanes 1 and 3), indicating that the accessibility of the Cys side chain to NEM is not dependent on thermal motion of the protein. No ligand-induced change in labeling of mutant G46C is apparent at 4 °C (Figure 2, compare lanes 1 and 2). It is essential to note that alkylation of sulfhydryl groups with NEM is rapid at 25 °C, given a reaction time of 10 min. With a sterically accessible thiol group, as in G46C permease, the reactivity of the Cys residue is not decreased upon lowering the temperature of the reaction to 4 °C. Hence, any difference in labeling of a Cys residue at 4 °C relative to that at 25 °C can be ascribed to an alteration in the environment of the Cys side chain. With T45C or S53C permease, the marked increase in labeling observed at 25 °C in the presence of TDG is almost absent at 4 °C, which indicates that without protein thermal motion, the Cys side chain is not labeled even in the presence of ligand (Figure 2, compare lanes 1 and 2 with lanes 3 and 4 in the appropriate panel). Labeling of F49C permease at 4 °C is slightly lower than that observed at 25 °C, implying that polypeptide thermal motion makes a small contribution to reactivity/accessibility of the Cys at this position (Figure 2, F49C, compare lanes 1 and 3). Interestingly, in the presence of ligand, labeling of mutant F49C is comparable at 4 and 25 °C (Figure 2, compare lanes 2 and 4), suggesting that accessibility at position 49 is no longer influenced by protein thermal motion. As a result, TDG-induced enhancement in the labeling of F49C permease is more pronounced at 4 °C than at 25 °C (Figure 2, compare lanes 1 and 2 with lanes 3 and 4). Labeling of Q60C permease at 4 °C is slightly lower than that observed at 25 °C, although ligand-induced attenuation in labeling is comparable at both temperatures (Figure 2, Q60C, compare lanes 1 and 2 with lanes 3 and 4). Lowering the temperature of alkylation to 4 °C also results in decreased labeling of S67C or L70C permease (Figure 2, compare lanes 1 and 3 in the appropriate panels), which indicates that thermal motion contributes to the strong labeling observed at 25 °C. With S67C permease, no ligand-induced change in labeling is observed at 25 °C, but at 4 °C when protein thermal motion is minimized, there is a slight decrease in labeling in the presence of TDG (Figure 2, S67C, compare lanes 1 and 2 with lanes 3 and 4). With L70C permease, TDG does not induce any change in labeling at 4 °C (Figure 2, L70C, compare lanes 1 and 2).

Effect of $\Delta\mu_{\text{H}^+}$ on NEM Labeling. Imposition of $\Delta\mu_{\text{H}^+}$ across the membrane has been reported to alter the NEM reactivity of V315C or V331C permease (13). Therefore, NEM labeling of each mutant in helix II was examined in the absence or presence of a $\Delta\mu_{\text{H}^+}$ generated by ascorbate oxidation in the presence of phenazine methosulfate. No significant changes were observed (data not shown).

Accessibility to MTSES. The NEM-reactive single-Cys permease mutants were tested for accessibility to methanethiosulfonate ethylsulfonate (MTSES), a hydrophilic, membrane-impermeant sulfhydryl reagent (14, 20–22). Pretreatment of G46C, A67C, or L70C permease with MTSES in either the absence or the presence of TDG leads to a marked decrease in labeling by NEM, which indicates that positions 46, 67, and 70 are accessible to solvent and that ligand binding does not alter the solvent exposure of these positions (Figure 3, appropriate panels). Labeling of permease mutants T45C or S53C by NEM after preincubation with MTSES in the

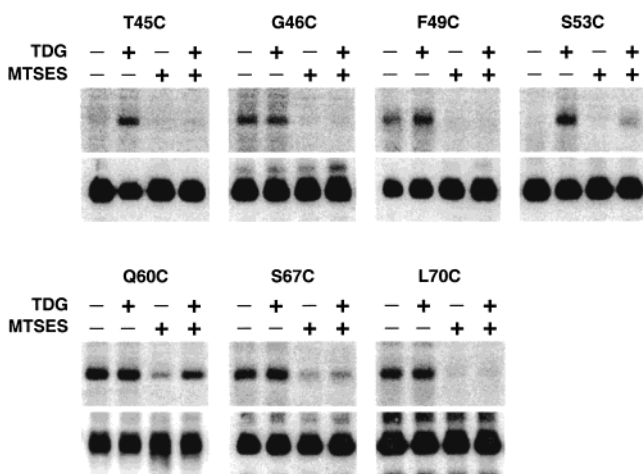


FIGURE 3: Accessibility of given single-Cys permease mutants to MTSES and the effect of TDG. RSO membrane vesicles (0.5–0.6 mg of protein in 0.5 mL of 100 mM KP_i (pH 7.5)/10 mM $MgSO_4$) prepared from *E. coli* T184 transformed with plasmid encoding the indicated single-Cys mutant were incubated without or with MTSES (200 μ M final concentration) for 5 min at 25 °C in the absence or presence of TDG (10 mM, final concentration), as indicated. The vesicles were washed twice with ice-cold buffer and resuspended in 50 μ L of the same buffer, and TDG (10 mM final concentration) was added back to the samples initially treated with TDG. The samples were then treated with [14 C]NEM (40 mCi/mmol; 0.4 mM final concentration) for 30 min at 25 °C. Reactions were quenched with DTT, and biotinylated permease was solubilized and purified as described in Experimental Procedures. Aliquots containing approximately 5 μ g of protein were separated by NaDodSO₄/12% PAGE, and the NEM-labeled protein was visualized by autoradiography (upper panels). A fraction of the protein (0.5 μ g) eluted from the avidin-Sepharose beads was analyzed by Western blotting with anti-C-terminal antibody to quantify the amount of permease in each sample (lower panels).

presence of TDG is almost nil, demonstrating that ligand binding not only causes these Cys side chains to become reactive but also leads to solvent exposure (Figure 3, appropriate panels). No labeling with NEM is evident when F49C permease is treated with MTSES in either the absence or the presence of TDG, indicating that position 49 is accessible to solvent independent of ligand binding (Figure 3, panel F49C). Treatment with MTSES also causes a pronounced decrease in labeling of Q60C permease, showing that the Cys side chain at position 60 is exposed to solvent (Figure 3, Q60C, compare lanes 1 and 3). Interestingly, pretreatment with MTSES in the presence of TDG causes partial restoration of NEM labeling, indicating that position 60 becomes less accessible to solvent upon ligand binding (Figure 3, compare lanes 3 and 4).

DISCUSSION

Cys-scanning mutagenesis of helix II and the flanking loops has identified nine positions where Cys substitution followed by treatment with NEM significantly decreases activity (1). The finding that 8 of the 9 NEM-sensitive positions are located on one face of helix II (Figure 4) suggests that this face may be involved in conformational changes important for turnover. In the present study, alkylation of 13 single-Cys permease mutants *in situ*, including the nine NEM-sensitive Cys-replacement mutants, was undertaken to further study this face of helix II. Modification of a given single-Cys residue in the permease by NEM clearly indicates that the thiol-containing side chain is

accessible to this relatively small, membrane-permeant reagent. Accessibility and/or reactivity may be determined by tertiary structure, thermal motion of the protein, and steric constraints imposed by the lipid bilayer and/or local environment, thereby providing structural information. Moreover, a change in reactivity/accessibility toward thiol reagents brought about by ligand binding or $\Delta\mu_H^+$ is generally indicative of an alteration in the local environment around the Cys residue of interest and provides a convenient means to detect conformational changes within the protein (13–15).

Mutants G46C, F49C, Q60C, S67C, and L70C are alkylated by NEM at 25 °C. However, the low reactivity of mutants G46C and F49C relative to the high reactivity of Q60C, S67C, and L70C suggests that Cys residues in the periplasmic half of helix II may be less accessible to NEM relative to Cys residues in the cytoplasmic half. Possibly, tertiary contacts between helix II and neighboring helices (23) are tighter in the periplasmic than in the cytoplasmic half. Mutants T45C and S53C react with NEM only in the presence of substrate, while I52C, S56C, L57C, L62C, F63C, and L65C permeases that contain Cys residues in the middle of the transmembrane domain do not react. Except for positions 56 and 63, which are located on the NEM-sensitive face of helix II, positions 52, 57, 62, and 65 lie on or close to the opposite, hydrophobic face, which may be embedded in the hydrocarbon phase of the membrane and/or in close opposition to hydrophobic faces of neighboring helices. Tertiary contacts within the protein or with the lipid bilayer may disfavor sterically and/or electronically alkylation of the Cys residue in these mutants. In any case, it is not clear why mutants S56C and L65C, which were reported to be inactivated by NEM (1), are not labeled. However, it is noteworthy that the NEM inactivation studies were carried out with intact cells and 1 mM NEM, while the labeling studies reported here were performed with RSO vesicles and 0.4 mM [14 C]NEM.

Structural changes occurring within the permease upon substrate binding are manifest at certain positions on the NEM-sensitive face of helix II by altered reactivity toward the alkylating agent (Figure 4). In the presence of TDG, Cys residues at positions 45 and 53 in the periplasmic half of the helix become reactive, the Cys at position 49 undergoes an increase in labeling, while Cys residues at positions 60 and 67 in the cytoplasmic half of the helix undergo a decrease in labeling. The results indicate that the face of helix II with positions 45, 49, 53, 60, and 67 participates in structural changes induced by ligand binding and support the conclusion (1, 3, 5, 6) that this face of helix II is important for conformational changes that occur during protein turnover.

Thermal motion of the protein which contributes to the structural flexibility of the permease may mask ligand-induced alterations in the reactivity/accessibility of single-Cys replacement residues toward sulfhydryl reagents. Decreasing the temperature of the alkylation reaction to 4 °C minimizes polypeptide motion, thereby enabling detection of ligand-induced conformational changes, particularly with mutants strongly labeled by NEM. With S67C permease, a small ligand-induced decrease in labeling that is not apparent at 25 °C becomes discernible at 4 °C. Similarly, mutant F49C exhibits a significantly greater substrate-induced increase in labeling at 4 °C than at 25 °C. In contrast, mutants T45C

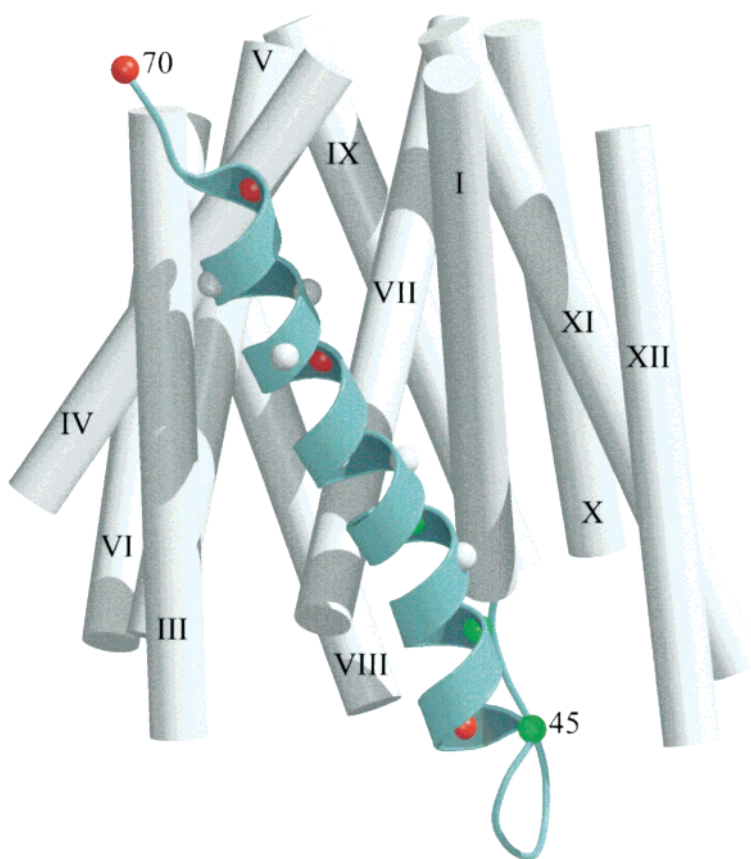


FIGURE 4: NEM labeling and the effect of ligand on single-Cys replacements in helix II. The results from Figure 2 are shown in a 3D representation of helix II as follows. Positions that label with NEM are presented as colored spheres: red, labels with NEM with no change in the presence of TDG; green, increased labeling in the presence of TDG; and blue, decreased labeling in the presence of TDG. Positions that do not label are shown as white spheres. Helices other than helix II are shown as rods, and their positions are derived from modeling studies (38) using approximately 100 constraints (23).

and S53C, which label with NEM at 25 °C only in the presence of TDG, exhibit almost no labeling at 4 °C, which suggests that polypeptide thermal motion is largely responsible for the observed reactivity of the Cys at positions 45 and 53 in the presence of ligand. The contribution of protein thermal motion to alkylation is also evident in mutants Q60C, S67C, and L70C where the extent of labeling at 4 °C is lower than at 25 °C. On the other hand, comparable reactivity of G46C permease at the two temperatures suggests that accessibility of the Cys side chain to NEM is independent of protein dynamics.

Site-directed thiol cross-linking studies (4–6, 24) show that the cytoplasmic halves of helices II and XI are in close proximity, while helices II and VII are close to each other at the periplasmic side of the membrane. Furthermore, TDG binding causes a scissors-like or translational movement of helices VII and/or II that increases the distance between helices VII and II at the periplasmic ends and decreases the distance at the approximate middle of the helices. An increase in distance between helices VII and II may increase accessibility of residues located at this interface to thiol reagents. Consistently, in the presence of TDG, there is marked enhancement of NEM labeling of Cys residues at positions 45, 49, and 53 located at the interface between helices II and VII. Similar increases in labeling in the presence of TDG are also observed with Cys residues at positions 241, 242, and 245 in the periplasmic half of helix VII at the same interface (Venkatesan, P., Kwaw, I., Hu, Y., and Kaback, H. R., preceding paper in this issue). However, these residues

in helix VII are highly reactive/accessible to NEM at 25 °C, and ligand-induced conformational changes at positions 241, 242, and 245 become apparent only when alkylation is performed at 4 °C. In contrast, Cys residues at positions 45, 49, and 53 in helix II exhibit a low degree of labeling at 25 °C, and conformational changes elicited by substrate binding are apparent at this temperature. Thermal motion of the protein appears to be primarily responsible for the pronounced reactivity/accessibility of the Cys side chains at positions 241, 242, and 245 at 25 °C, but in the presence of ligand, labeling at these positions is not determined by protein dynamics. Likewise, thermal motion makes a small contribution to the reactivity of the Cys residue at position 49, although labeling in the presence of TDG is not affected by protein dynamics. The Cys side chains at positions 45 and 53 behave differently from the other Cys replacements at the helix II/VII periplasmic interface. Neither mutant is labeled, and labeling observed in the presence of ligand appears to stem from thermal motion. Thus, despite spatial proximity, the periplasmic halves of helices II and VII have distinct properties conferred by tertiary structure, thermal motion of the protein, and/or constraints imposed by the bilayer.

Two-thirds of helix II forms a continuous hydrophobic face composed mostly of Leu, Phe, Ile, and Ala residues that probably face the interior of the bilayer (23). Most Cys-replacement mutants on this face exhibit good transport activity, and with the exception of L65C, none are markedly inhibited by NEM (1). The present study shows that the

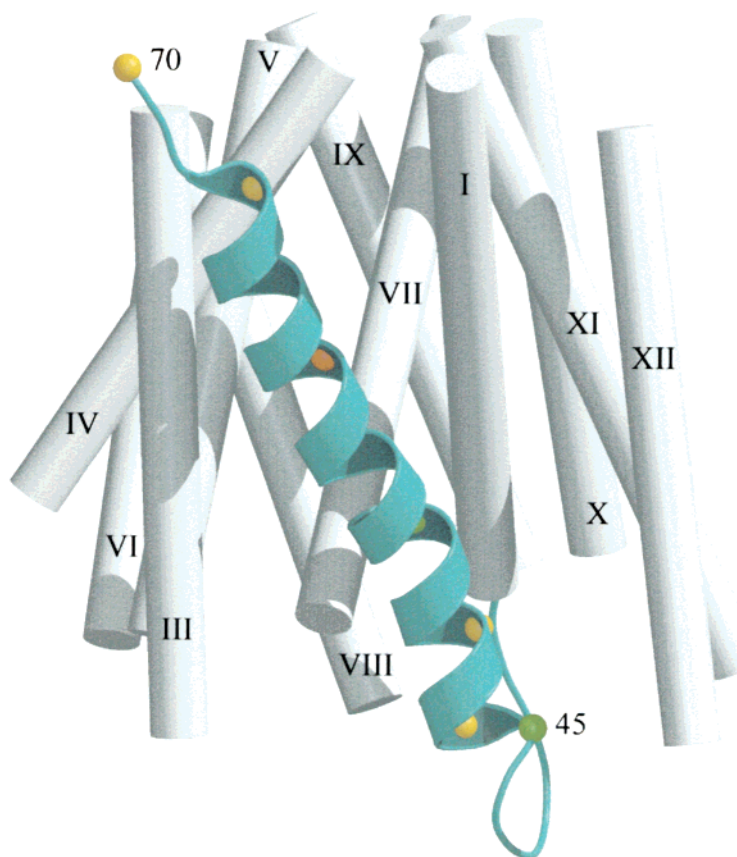


FIGURE 5: Solvent accessibility of single-Cys replacements in helix II as judged by MTSES blockade of NEM labeling. Results from Figure 3 are shown in a 3D representation of helix II. Positions where NEM labeling is significantly blocked by MTSES are shown as yellow spheres. Positions 45 and 53 are represented as green spheres to indicate increased accessibility to solvent in the presence of TDG; position 60 is represented as an orange sphere to indicate a ligand-induced decrease in accessibility. Helices other than helix II are shown as rods, and their positions are derived from modeling studies (38) using approximately 100 constraints (23).

remaining third of the transmembrane face of helix II containing NEM-sensitive positions is exposed to solvent. Labeling of all the single-Cys replacements on this face with NEM is blocked by MTSES, indicating that this face is accessible to periplasmic solvent throughout the thickness of the membrane (Figure 5). Cys residues at positions 45 and 53 become accessible to MTSES in the presence of TDG, while those at positions 46, 49, 67 (located at the cytoplasmic end of helix II; Figure 1), and 70 (loop II/III) are accessible to MTSES in the absence or presence of ligand. The Cys at position 60 is also exposed to solvent, and TDG binding results in a decrease in the solvent accessibility of the Cys at this position. Although the conclusion that one face of helix II appears to be accessible to periplasmic solvent throughout the thickness of the membrane may seem heretical, the permease is a very flexible molecule (25) in which the backbone is highly accessible to water despite its overall hydrophobic nature (26). Furthermore, a large body of evidence demonstrates that there is little if any contamination of RSO vesicle preparations with either leaky or inverted vesicles (27–32), and as shown in Figure 3, MTSES blocks NEM labeling almost completely with either S67C or L70C permease. Since the cytoplasmic end of helix II cross-links to the cytoplasmic end of helix XI, it is also unlikely that loop II/III re-enters the membrane to form a P loop.

In summary, the findings presented here suggest that the membrane spanning, hydrophilic face of helix II containing Gly46, Phe49, Ser53, Gln60, and Ser67 may form part of the solvent-filled cleft in the permease visualized by electron

microscopy (33–37). It may also be highly significant that the solvent-accessible face of helix II reflects structural changes induced by substrate binding, especially if the water-filled cleft represents the translocation pathway through the permease.

ACKNOWLEDGMENT

We are deeply indebted to Mark Girvin for molecular modeling. In addition, we thank Kerstin Stempel for help with the preparation of the figures.

REFERENCES

1. Frillingos, S., Sun, J., Gonzalez, A., and Kaback, H. R. (1997) *Biochemistry* 36, 269–273.
2. Jessen-Marshall, A. E., Paul, N. J., and Brooker, R. J. (1995) *J. Biol. Chem.* 270, 16251–16257.
3. Jessen-Marshall, A. E., and Brooker, R. J. (1996) *J. Biol. Chem.* 271, 1400–1404.
4. Wu, J., and Kaback, H. R. (1996) *Proc. Natl. Acad. Sci. U.S.A.* 93, 14498–14502.
5. Wu, J., and Kaback, H. R. (1997) *J. Mol. Biol.* 270, 285–293.
6. Wu, J., Hardy, D., and Kaback, H. R. (1998) *J. Mol. Biol.* 282, 959–967.
7. Sun, J., and Kaback, H. R. (1997) *Biochemistry* 36, 11959–11965.
8. Sun, J., Kemp, C. R., and Kaback, H. R. (1998) *Biochemistry* 37, 8020–8026.
9. Sun, J., Voss, J., Hubbell, W. L., and Kaback, H. R. (1999) *Biochemistry* 38, 3100–3105.

10. Henderson, P. J. (1990) *J. Bioenerg. Biomembr.* 22, 525–569.
11. McKenna, E., Hardy, D., and Kaback, H. R. (1992) *Proc. Natl. Acad. Sci. U.S.A.* 89, 11954–11958.
12. Jung, K., Jung, H., Colacurcio, P., and Kaback, H. R. (1995) *Biochemistry* 34, 1030–1039.
13. Frillingos, S., and Kaback, H. R. (1996) *Biochemistry* 35, 3950–3956.
14. Frillingos, S., and Kaback, H. R. (1997) *Protein Sci.* 6, 438–443.
15. Frillingos, S., Wu, J., Venkatesan, P., and Kaback, H. R. (1997) *Biochemistry* 36, 6408–6414.
16. Consler, T. G., Persson, B. L., Jung, H., Zen, K. H., Jung, K., Prive, G. G., Verner, G. E., and Kaback, H. R. (1993) *Proc. Natl. Acad. Sci. U.S.A.* 90, 6934–6938.
17. Sanger, F., Nicklen, S., and Coulson, A. R. (1977) *Proc. Natl. Acad. Sci. U.S.A.* 74, 5463–5467.
18. Konings, W. N., Barnes, E. M., Jr., and Kaback, H. R. (1971) *J. Biol. Chem.* 246, 5857–5861.
19. Careaga, C. L., and Falke, J. J. (1992) *J. Mol. Biol.* 226, 1219–1235.
20. Akabas, M. H., Stauffer, D. A., Xu, M., and Karlin, A. (1992) *Science* 258, 307–310.
21. Stauffer, D. A., and Karlin, A. (1994) *Biochemistry* 33, 6840–6849.
22. Karlin, A., and Akabas, M. H. (1995) *Neuron* 15, 1231–1244.
23. Kaback, H. R., and Wu, J. (1999) *Acc. Chem. Res.* 32, 805–813.
24. Wu, J., Hardy, D., and Kaback, H. R. (1998) *Biochemistry* 37, 15785–15790.
25. le Coutre, J., Narasimhan, L. R., Patel, C. K., and Kaback, H. R. (1997) *Proc. Natl. Acad. Sci. U.S.A.* 94, 10167–10171.
26. le Coutre, J., Kaback, H. R., Patel, C. K. N., Heginbotham, L., and Miller, C. (1998) *Proc. Natl. Acad. Sci. U.S.A.* 95, 6114–6117.
27. Kaback, H. R. (1971) *Methods Enzymol.* 22, 99–120.
28. Short, S. A., Kaback, H. R., Kaczorowski, G., Fisher, J., Walsh, C. T., and Silverstein, S. C. (1974) *Proc. Natl. Acad. Sci. U.S.A.* 71, 5032–5036.
29. Short, S. A., Kaback, H. R., and Kohn, L. D. (1975) *J. Biol. Chem.* 250, 4291–4296.
30. Owen, P., and Kaback, H. R. (1978) *Proc. Natl. Acad. Sci. U.S.A.* 75, 3148–3152.
31. Owen, P., and Kaback, H. R. (1979) *Biochemistry* 18, 1413–1422.
32. Owen, P., and Kaback, H. R. (1979) *Biochemistry* 18, 1422–1426.
33. Costello, M. J., Viitanen, P., Carrasco, N., Foster, D. L., and Kaback, H. R. (1984) *J. Biol. Chem.* 259, 15579–15586.
34. Costello, M. J., Escaig, J., Matsushita, K., Viitanen, P. V., Menick, D. R., and Kaback, H. R. (1987) *J. Biol. Chem.* 262, 17072–17082.
35. Li, J., and Tooth, P. (1987) *Biochemistry* 26, 4816–4823.
36. Li, J., and Tooth, P. (1988) *Prog. Clin. Biol. Res.* 273, 93–98.
37. Zhuang, J., Privé, G. G., Verner, G. E., Ringler, P., Kaback, H. R., and Engel, A. (1999) *J. Struct. Biol.* 125, 63–75.
38. Rastogi, V. K., and Girvin, M. E. (1999) *Nature* 402, 263–268.

BI0004394